Underwater 3-D Spatial Attenuation Characteristics of Electromagnetic Waves With Omnidirectional Antenna

Kyungmin Kwak, *Student Member, IEEE*, Daegil Park, *Student Member, IEEE*, Wan Kyun Chung, *Fellow, IEEE*, and Jinhyun Kim, *Member, IEEE*

***Abstract*—In this paper, an underwater 3-D spatial attenuation model of electromagnetic waves is proposed to establish a position recognition system in underwater 3-D space using distance estimation. The distance estimation is based on signal attenuation characteristics of electromagnetic waves radiated through several omnidirectional antennas. Positions in underwater environments have been predominantly estimated by an ultrasonic position recognition system using travel time and phase difference. However, such a system provides inaccurate estimation on account of the multipath effect in a structured environment or complex environment with many obstacles. A position estimation method that uses signal attenuation of electromagnetic waves has been proposed to overcome this limitation. That method can precisely estimate position on a structured 2-D plane. In this paper, an existing underwater position estimation system based on electromagnetic waves is expanded into 3-D space using the Friis formula and plane wave equation, thereby classifying attenuation characteristics of electromagnetic waves into the effects of medium, radiation, and antenna. These effects are summarized to deduce the signal attenuation characteristics of electromagnetic waves in 3-D space. In addition, the relative position (R, Θ, Φ) and attitude (ϕ, θ, ψ) of transceiver antennas are used to define a coordinate system for 3-D estimation; moreover, an attenuation model is defined for individual factors in the coordinate system. A generalized attenuation model of an omnidirectional antenna in 3-D space is presented, and the validity of the proposed model is demonstrated through experiments. Based on the results, the proposed model demonstrates the potential application to an omnidirectional antenna and expansion into an attenuation model based on the 3-D position between random antennas.**

***Index Terms*—Electromagnetic waves, received signal strength (RSS), sensor network, underwater localization.**

Manuscript received April 30, 2015; revised September 23, 2015; accepted November 2, 2015. Date of publication January 14, 2016; date of current version April 28, 2016. This research was a part of the project titled "Development of small drag bio-mimetic underwater robots", funded by the Ministry of Oceans and Fisheries, Korea and by the Industrial Source Technology Development Programs of the Ministry Of Trade, Industry and Energy (MOTIE), Korea, under Grant 10043928. Recommended by Technical Editor X. Tan.

K. Kwak and J. Kim are with the Department of Mechanical Engineering, Seoul National University of Science and Technology, Seoul 01811, Korea (e-mail: supermaxx@seoultech.ac.kr; jinhyun@seoultech.ac.kr).

D. Park and W. K. Chung are with the Department of Mechanical Engineering, Pohang University of Science and Technology, Pohang 37673, Korea (e-mail: daegilpark@postech.ac.kr; wkchung@postech.ac.kr).

Color versions of one or more of the figures in this paper are available online at http://ieeexplore.ieee.org.

Digital Object Identifier 10.1109/TMECH.2015.2509466

I. Introduction

There have been many recent efforts to develop marine systems that require the use of marine resources. The unmanned underwater vehicle (UUV), which is used in environments that are risk prone or that restrict human access, is a representative example. For example, track-type underwater robots are used to bury power and communication cables [1], and free-floating underwater robots are used to remove mines and for exploration [2], [3]. A UUV was sent to an underwater depth of 1500 m during the crude oil spill in the Gulf of Mexico to repair the damaged well [4].

An ability to examine the relative or absolute position of a robot is required for its use in underwater environments; therefore, many studies have been conducted to estimate its underwater position [5], [6]. Methods include finding the distance between nodes installed in geographic features or ships using time or angle of arrival (TOA, AOA) for reflection of ultrasonic waves based on a Doppler velocity log (DVL) and side-scan sonar [7]; finding the position by detecting a mark at a specific point using an optical (vision) sensor [8]; and using distance estimation with underwater signal attenuation of electromagnetic waves [9]. Among these methods, the DVL [7] and baseline system, which employ ultrasonic waves with excellent underwater transfer performance, are the most widely used.

DVL is used in ultrasonic self-navigation to estimate the velocity and direction vector according to the movement of vehicles and the phase difference of ultrasonic waves reflected from the seabed. This method examines the movement of robots relative to the current position; moreover, it includes an information-update cycle of several hertz. DVL estimates the new position and direction relative to the current position, whereas the baseline technique estimates the relative position of robots around a node with a fixed position using the phase difference, TOA, or AOA of ultrasonic waves. Ultrasonic position estimation is a widely used verified system for estimating the relative position of the robot from a ship in a wide range. However, because underwater ultrasonic waves incur the multipath effect in shallow water environments or in areas installed with complex structures, estimation precision is reduced or incorrect information may be obtained [10]. Furthermore, ultrasonic waves cannot be used for close distance works involving manipulators and work tools, such as for construction of structures that require a high degree of precision. As an alternative, studies have been conducted on a technique that estimates the underwater position in a structured environment or at a near distance using signal

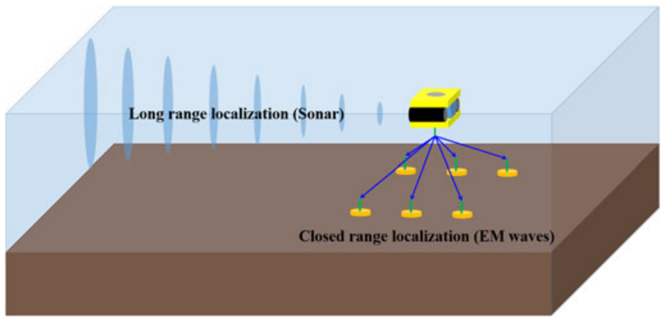

Fig. 1. Conceptual diagram of EM waves and sonar combined in a localization system.

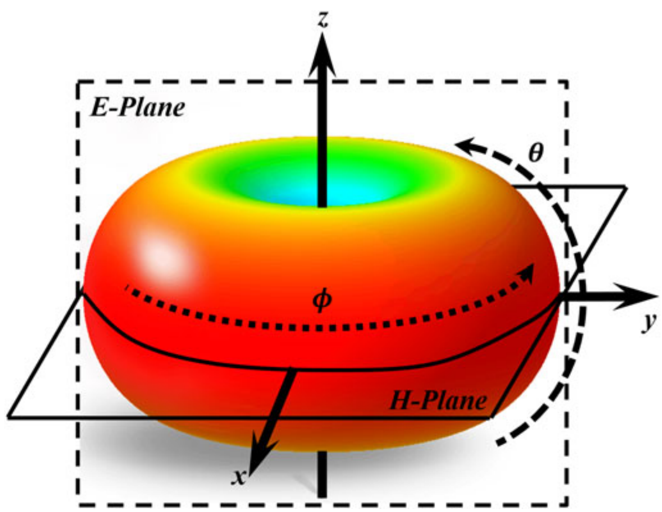

Fig. 2. Attenuation pattern of omnidirectional antenna.

attenuation of electromagnetic waves. Other studies were performed on signal attenuation based on distance and the medium of electromagnetic waves [11]–[13]. Furthermore, a study was conducted on the underwater distance attenuation model and 2-D position recognition [14]. The results of these studies in experimental water basins verified that position can be precisely estimated using electromagnetic waves to approximately several centimeters. Unlike existing position estimation systems based on ultrasonic waves, the electromagnetic-wave-based system can be used in an environment that requires precise estimation at a close distance. Hence, EM waves and sonar combined in a localization system can extend its range and improve its precision, as shown in Fig. 1.

However, position estimation using attenuation of electromagnetic waves has only been performed on a 2-D plane with the H-plane attenuation model of an omnidirectional antenna, as shown in Fig. 2. No signal attenuation model has been developed based on the difference in relative height and attitude of antennas, which are E-plane characteristics required for 3-D estimation. As shown in Fig. 2, the radiation characteristics of the omnidirectional antenna are proximate to an epicenter in accordance with the distance on the horizontal H-plane. The vertical E-plane, on the other hand, does not show a fixed pattern in accordance with the distance; consequently, further research is needed.

In this study, therefore, modeling was performed on the signal attenuation of electromagnetic waves for antennas positioned at respective fixed and mobile nodes to establish a 3-D underwater position estimation system using electromagnetic waves. The coordinate system was defined for the modeling of attenuation patterns based on the relative position and attitude between nodes, and an attenuation model was defined for each factor. A generalized 3-D signal attenuation model for an omnidirectional antenna was proposed, and the effectiveness of this model was verified through experiments.

The major contributions of this paper are as follows. First, a generalized attenuation model is defined based on the existing Friis formula and plane wave equation in Section II. The position loss factor and attitude loss factor are defined using the spherical coordinate system and Euler angles according to the relative position and attitude of the transceiver antenna (fixed node and mobile node) in Section III-A. Second, a model is defined based on the distance (R) and elevation angle (Θ) between two nodes among components of the position loss factor in Section III-B. In addition, attenuation factors are defined according to roll (ϕ) and pitch (θ) of the attitude loss factor based on changes in the attitudes of mobile nodes in Section III-C. Furthermore, the effects of medium, radiation, and antenna in terms of the omnidirectional antenna in the generalized attenuation model are formulated with the position loss factor and attitude loss factor for the proposed system model for 3-D underwater attenuation in Section III-D. Finally, the several experiments performed on the proposed 3-D underwater attenuation model using the omnidirectional antenna, as well as the verification of the model by comparative analysis, are described in Section IV.

II. Attenuation Factors of Electromagnetic Waves

Attenuation based on the transmitting and receiving electromagnetic waves is determined by the medium through which the electromagnetic waves pass, the radiation of the electromagnetic waves, and the resonance area according to the antenna characteristics. First, (1), proposed by Maxwell [15] and A. Karlsson [16], indicates that attenuation based on the medium exponentially occurs by distance (R) based on attenuation constant α

$$\frac{P_R}{P_T} = e^{-\alpha R}. \tag{1}$$

Here, P_T is transmitted energy and P_R is receiving energy. Attenuation constant α is defined by conductivity σ, permeability μ, and permittivity ϵ, as shown in (2). Conductivity is the degree to which electricity flows in a conductive medium based on the number of free electrons distributed inside the medium. Permeability is the degree to which magnetic flux passes through a medium or interior of a material. Permittivity is the ratio by which an electric field inside a dielectric material is weakened when another electric field is created by polarization in the direction opposite the electric field passing through the dielectric material. The attenuation ratio of electromagnetic waves passing through a medium is determined by the attenuation constant, which involves three constants [15]

$$\alpha = \omega\sqrt{\epsilon\mu}\sqrt{\frac{1}{2}\left[\sqrt{1+\frac{\sigma^2}{\omega^2\epsilon^2}}-1\right]} \tag{2}$$

where ω is a radian frequency of the electromagnetic wave.

In addition to the medium effect, the energy density of electromagnetic waves decreases when the distance is increased by radiation. Signal attenuation of electromagnetic waves additionally results from characteristics of the transmitting and receiving antennas. The Friis formula represents these phenomena. The proposed attenuation model of electromagnetic waves using the Friis formula is shown as [17]

$$\frac{P_R}{P_T} = \frac{\lambda^2}{4\pi R^2} G_T G_R (\text{PLF}). \tag{3}$$

This model consists of gains that represent the performances of transmitting and receiving antennas G_T, G_R, wavelength λ of the electromagnetic waves, the distance between transmitting and receiving antennas R, the polarization loss factor (PLF), and the intensity of transmitting and receiving waves P_T, P_R. In sum, the attenuation of transmitting and receiving energies according to the Friis formula is affected by the attenuation of the radiation area based on the change in distance between the antennas, the gain that represents the antenna performance, and the PLF caused by the dislocation of wave propagation angles between the antennas.

The distance between the antennas and the PLF in the above model are determined by the position and attitude of two antennas; however, the gain pattern of the antennas greatly differs according to the antennas used. The gain pattern of antennas is generally expressed by connecting the points at which the same energy density is shown by electromagnetic waves. Theoretically, the gain is an effect in which the energy density distribution is differentiated according to the antenna when the total energy is maintained as constant. However, the Friis formula does not provide a detailed analysis about the effect of antenna gain. An antenna gain can be handled as a constant because it is the same in all directions in 3-D space when isotropic antennas are used. Nonetheless, the antenna gain effect must be considered because, in reality, it is difficult to make isotropic antennas; moreover, the 3-D environment is greatly affected by the antenna gain pattern based on the relative position of the antennas. For example, omnidirectional dipole antennas produce a doughnut-shaped gain pattern [18]. Unlike isotropic antennas that show the same signal attenuation at the same distance when the transmitting and receiving antennas are vertically aligned, such as the node "a" shown in Fig. 3, omnidirectional dipole antennas may be unable to receive any signals. Therefore, the effect of radiation, antenna gain, and relative attitude between antennas must be considered for the embodiment of a more accurate model of signal attenuation of electromagnetic waves.

A generalized model applicable to all antennas is defined as (4) by classifying the attenuation of electromagnetic waves between two omnidirectional antennas into attenuation by medium, attenuation by radiation, and attenuation by antenna properties, such as position and attitude

$$\frac{P_R}{P_T} = F_{\text{Medium}} \times F_{\text{Radiation}} \times F_{\text{Antenna property}}. \tag{4}$$

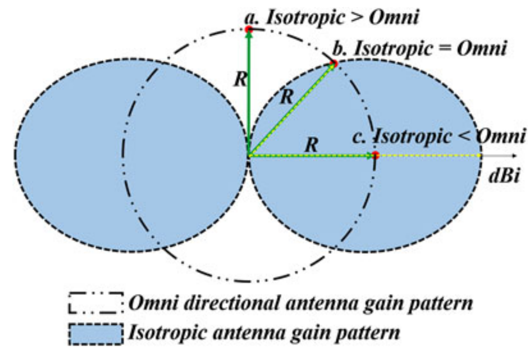

Fig. 3. Gain comparison between isotropic and omnidirectional antennas.

To complete such a generalized model in terms of 3-D estimation, a generalized model is proposed in Section III that can be actually used by theoretically analyzing attenuation patterns on the horizontal radiation plane (H-plane) and vertical radiation plane (E-plane). Although (4) can be defined by the Friis formula and the plane wave equation in the case of ideal isotropic antennas, isotropic antennas cannot exist in reality. For this reason, the detailed modeling of omnidirectional antennas, the most appropriate type of antenna for a position sensor, is described in this paper.

III. Study on Attenuation Pattern of Electromagnetic Waves With Omnidirectional Antenna

The generalized signal attenuation model of (4) addresses attenuation factors. The effects of these factors on overall signal attenuation are explained in this section.

A. Coordinate System

First, the 3-D attenuation pattern of electromagnetic waves must be examined for easier understanding of change in signal attenuation in all directions. The movements of transmitting and receiving nodes (fixed and mobile nodes) that affect each attenuation factor must be defined. The spherical coordinate system [19] is utilized with consideration of the radiation characteristics of electromagnetic waves to define attenuation for 3-D position factors.

The spherical coordinate system is the most appropriate coordinate system for defining attenuation factors according to distance and radiation of electromagnetic waves because it expresses the coordinates in terms of distance (R), which is one attenuation factor of electromagnetic waves. The attenuation effect based on the relative position between a fixed node and mobile node is defined as the position loss factor. As shown in Fig. 4, the position between nodes is represented by distance R, angle of rotation Φ, and elevation angle Θ. In addition, as shown in Fig. 5, the attitude loss factor is defined as an attenuation factor based on the change in mobile node attitude. The

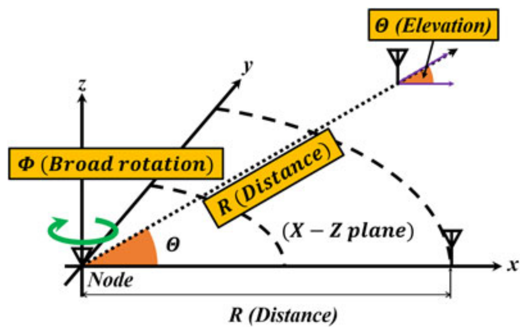

Fig. 4. Components of position loss factor.

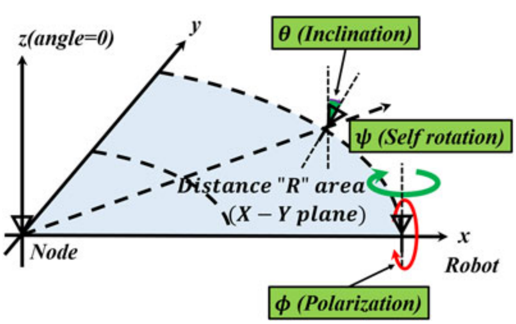

Fig. 5. Components of attitude loss factor.

attitude loss factor shows attenuation according to roll, pitch, and yaw using the Euler angle (*zyx* convention) between two nodes. Roll angle is defined as polarization ϕ between antennas, pitch angle is denoted as inclination θ, and yaw angle as ψ.

In ideal isotropic antennas, attenuation only occurs according to distance and polarization angle regardless of attitude discordance; the other four factors do not need to be considered. Because omnidirectional antennas have the same attenuation pattern in all directions on the H-plane, it is not necessary to consider the effects of the position loss factor on the angle of rotation (Φ), and that of the attitude loss factor on yaw angle (ψ), when omnidirectional antennas are used for both transmission and reception. The next section defines attenuation factors according to the relative positions of nodes, and a model for individual attenuation factors is presented.

B. Position Loss Factor

As shown in Fig. 4, position loss factor can be expressed by attenuation function $F(R)$ based on the distance between nodes and by attenuation function $F(\Theta)$ based on elevation angle. Signal attenuation function $F(R)$ based on distance can be expressed as shown below with attenuation based on the medium using the Friis formula and plane wave equation, which are, respectively, based on transmitted energy density and receiving area [12]

$$F(R) = \frac{\lambda^2}{4\pi R^2} e^{-\alpha R}. \tag{5}$$

When transmitting and receiving antennas are omnidirectional antennas, the attenuation pattern on the horizontal plane according to distance is the same in all directions when there is no angle rotation and the two antennas are maintained in parallel.

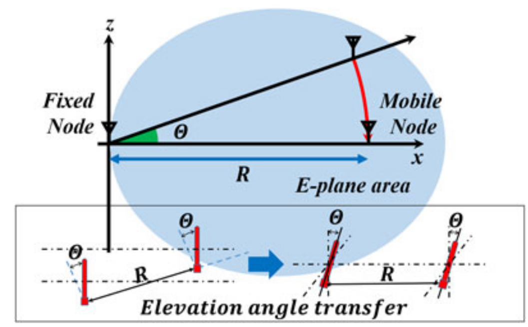

Fig. 6. Definition of elevation angle.

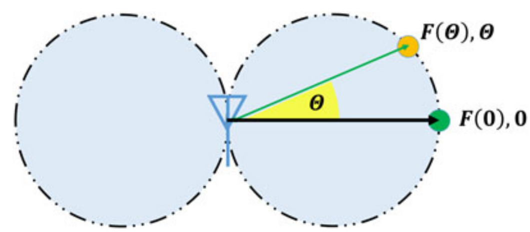

Fig. 7. Concept of antenna elevation function.

This can be expressed as (5). However, a change in the vertical positions of antennas must be considered in 3-D space. Signal transmission and reception points can be dislocated by the difference in vertical position between the two antenna nodes in a 3-D environment; the attenuation factor must be defined accordingly. The attenuation factor for angle change based on the vertical position is expressed as elevation angle (Θ); its attenuation effect is defined as the elevation loss factor. Elevation loss factor refers to the rotation angle based on the z-axis movement in the same distance as the mobile node compared to the fixed node, which can be expressed as shown in Fig. 6. In addition, when two antennas located on the x-axis are rotated to the same angle, they show the same effect as the elevation angle. This method enables easy elevation angle experimentation, as shown by the experiment described in Section IV.

The attenuation effect of omnidirectional transmitting and receiving antennas according to elevation angle Θ can be shown by attenuation based on the distance between the antenna and measurement point and elevation angle, as shown in Fig. 7. Based on the omnidirectional antenna pattern model, attenuation based on elevation angle shown in Fig. 7 yields a value attenuated by the pattern model of the antenna compared to the value when $\Theta = 0$.

Under the premise that the gain pattern model for the vertical plane of each omnidirectional antenna constituting the elevation angle has a fixed distance, the distance can be expressed in accordance with the change in vertical position of the single antenna using maximum directivity $D_{\max}$ when transmitting and receiving antennas are at the same vertical position ($\Theta = 0$) and pattern model $U_{\text{Elevation}}$ as [17]

$$D(\Theta) = D_{\max} \times U_{\text{Elevation}}. \tag{6}$$

First, the maximum directivity of (6) can be expressed using the half-power beam width (HPBW) as in (7). HPBW refers to the angle formed by two points at which the signal intensity

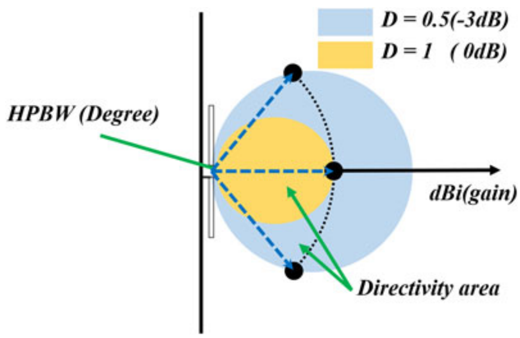

Fig. 8. Definition of HPBW.

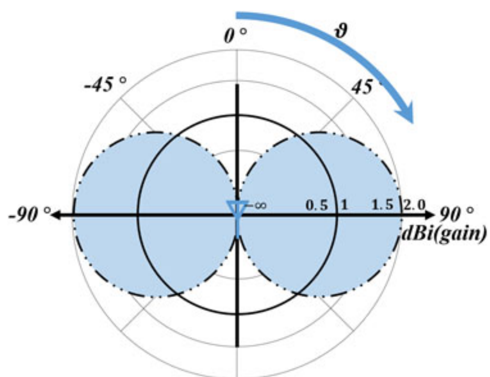

Fig. 9. Omnidirectional antenna radiation pattern.

corresponds to -3 dB (0.5 times) the maximum signal intensity when the receiving antenna is rotated around the transmitting antenna at the same distance as in Fig. 8. This assumes that the two antennas are positioned on the same horizontal plane and the point of maximum reception signal intensity is 1

$$D_{\max} = \frac{101}{\mathrm{HPBW} - 0.0027(\mathrm{HPBW})^2} \tag{7}$$

where HPBW should be used as a degree value.

The directivity of the antenna in (6) is explained with the maximum directivity in (7) and the pattern model of the omnidirectional antenna. Equation (7) is a model of the maximum directivity proposed by McDonald based on a mathematical experimental model [17]. This model can determine the maximum directivity of the antenna using HPBW. The pattern model for the vertical position of the antenna is the model that is required when the position movement occurs with the same distance as that of the transmitting and receiving antennas on the *xz* plane, as shown in Fig. 6. The pattern model for the omnidirectional antenna is required to examine this model. The omnidirectional antennas have pattern characteristics shown by the 2-D pattern in Fig. 9. Such patterns can be approximated by [17]

$$U = |\sin^n(\vartheta)|, \quad 0 < \vartheta < 2\pi. \tag{8}$$

When the pattern model for the antenna of (8) is applied to the pattern model according to the maximum gain of (7), the directivity model for a single antenna can be verified once again as

$$D = D_{\max} |\sin^n(\vartheta)|. \tag{9}$$

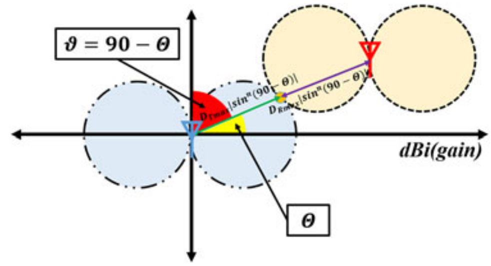

Fig. 10. EM waves resonance between transmitting and receiving antennas.

The generalized model for determining the directivity using the omnidirectional antenna pattern is verified in (9). To show this model as a directivity model according to a change in elevation angle ϑ, which corresponds to the radiation pattern of the antenna, must be defined as $90 - \Theta$, which is the angle of rotation from the *x*-axis. The corresponding model is presented by

$$D = D_{\max} |\sin^n(90 - \Theta)| = D_{\max} |\cos^n(\Theta)|. \tag{10}$$

In this paper, the attenuation model for the omnidirectional antenna according to rotation is verified using the directivity found in (10). This model can be used to show the attenuation pattern of the general omnidirectional antenna according to the angle of the E-plane as

$$\begin{aligned} F(\Theta) =& \; D_T(\Theta) D_R(\Theta) \\ =& \; |D_{T\max} \cos^{n_T} \Theta| \times |D_{R\max} \cos^{n_R} \Theta|. \end{aligned} \tag{11}$$

The signal attenuation factor of two antennas according to rotation is expressed as a product in (11). Based on the Friis formula, electromagnetic waves that leave the transmitting antenna resonate in the region of the receiving antenna. They are not only influenced by the directivity of the transmitting antenna but also by the receiving antenna directivity. This can be expressed as shown in Fig. 10.

Equation (11), expressed as a product on account of resonance, shows the model for two gains. Because two antennas identically rotate according to the elevation angle, as shown in Fig. 6, they can both be expressed using Θ.

C. Attitude Loss Factor

The attenuation factor of the position loss factor is caused by the difference in relative position between the two node antennas. The attenuation factor of the attitude loss factor results from the difference in the relative attitude of the mobile node antennas, as shown in Fig. 5. The effects of the two detailed factors, roll and pitch, must be analyzed to define attitude loss factor.

ϕ is the angle between the transmission and reception signal vectors. It can be expressed as the angle based on the mobile node rotation in the direction of the roll. As noted by PLF in the Friss equation, the roll rotation of the mobile node leads to the dislocation of the electric and magnetic fields that constitute the electromagnetic waves, thereby causing the attenuation effect. This can be defined as a factor of attitude loss factor $F(\phi)$

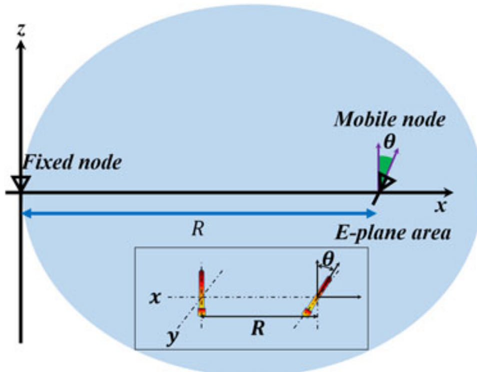

Fig. 11. Inclination loss factor: $F(\theta)$.

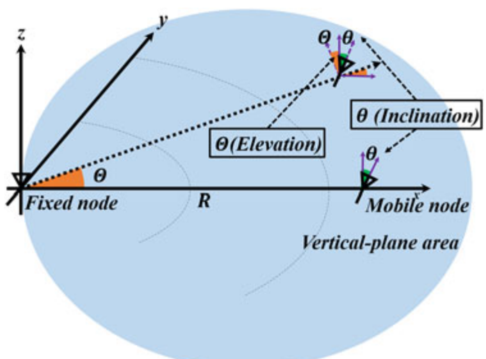

Fig. 12. Combined elevation and inclination loss factors $F(\Theta, \theta)$.

as follows (same equation with PLF in [17]):

$$F(\phi) = \cos^2(\phi). \tag{12}$$

Another factor is the attenuation effect based on the rotation angle in the direction of the pitch. As shown in Fig. 11, this can be regarded as the effect of pitch rotation of the mobile node compared to the fixed node. In this paper, it is defined as the inclination loss factor.

Inclination loss factor can be determined using the same method for elevation loss factor mentioned in the previous section. In other words, elevation loss factor refers to the attenuation caused by the simultaneous rotation of two antennas. Inclination loss factor can be explained as the attenuation caused by the rotation of a single antenna as

$$F(\theta) = |D_{T\max} \cos^{n_T}(0)| \times |D_{R\max} \cos^{n_R}(\theta)|. \tag{13}$$

A new model is additionally required when the elevation loss factor and inclination loss factor simultaneously occur, as shown in Fig. 12. It can be defined as

$$F(\Theta, \theta) = |D_{T\max} \cos^{n_T}(\Theta)| \times |D_{R\max} \cos^{n_R}(\Theta + \theta)|. \tag{14}$$

D. Generalized Omnidirectional Antenna Attenuation Model

Using the position loss factor and attitude loss factor as attenuation factors proposed in Sections III-B and III-C, a new model for a general 3-D radiation pattern of electromagnetic waves with an omnidirectional antenna can be proposed as (15).

TABLE I
COMPONENTS OF GENERALIZED EXTENDED FRIIS MODEL

$F(R)_{\text{Lossy medium}}$	$e^{-\alpha R}$
$F(R)_{\text{Radiation}}$	$\frac{\lambda^2}{4\pi R^2}$
$F(\phi)_{\text{Polarization}}$	$\cos^2(\phi)$
$F(\Theta, \theta)_{\text{Elevation and Inclination}}$	$\lvert D_{T\max}\cos^{n_T}(\Theta)\rvert \lvert D_{R\max}\cos^{n_R}(\Theta+\theta)\rvert$

Here, $e_T\, e_R$ is the efficiency according to the physical characteristics of the antennas, $(1 - |\Gamma_T|^2)(1 - |\Gamma_R|^2)$ is the efficiency according to the mismatching of impedance from penetration of different mediums, and $e^{-\alpha R}$ is attenuation according to medium and distance. In addition, $\lambda^2/4\pi R^2$ is the effect of the transfer energy of the transmitting antenna and the effective area of the receiving antenna, while $F(\phi, \Theta, \theta)$ is the attenuation factor according to the change in antenna position presented earlier

$$\frac{P_R}{P_T} = e_T e_R \times (1 - |\Gamma_T|^2)(1 - |\Gamma_R|^2) e^{-\alpha R} \times \frac{\lambda^2}{4\pi R^2} \times F(\phi, \Theta, \theta). \tag{15}$$

The proposed models can be applied to $F(\phi, \Theta, \theta)$ of (15) to be expressed as

$$\frac{P_R}{P_T} = e_T e_R \times (1 - |\Gamma_T|^2)(1 - |\Gamma_R|^2) e^{-\alpha R} \times \frac{\lambda^2}{4\pi R^2} \times \cos^2(\phi) \times |D_{T\max} \cos^{n_T}(\Theta)| \times |D_{R\max} \cos^{n_R}(\Theta + \theta)|. \tag{16}$$

Equation (17) is the generalized underwater 3-D model proposed in this paper for the omnidirectional antenna. This model can be applied to a medium other than an underwater environment depending on the value of the attenuation constant. However, experimental verification was only performed underwater, as described in Section IV. Because this model was devised for use in an underwater position recognition system, the scope of the model in this paper is limited to an underwater environment. The Friis model involves a restricted domain of free space, whereas this study considered attenuation in an underwater environment as a lossy medium. In addition, the omnidirectional antenna attenuation pattern is defined, and a model for the attenuation approximation according to the positions of the transmitting and receiving antennas is proposed. This can be summarized for each characteristic as shown in (17) and Table I

$$\begin{aligned}\frac{P_R}{P_T} = {} & e_T e_R \times (1 - |\Gamma_T|^2)(1 - |\Gamma_R|^2) \\ & \times F(R)_{\text{Lossy medium}} \times F(R)_{\text{Radiation}} \\ & \times F(\phi)_{\text{Polarization}} \\ & \times F(\Theta, \theta)_{\text{Elevation and Inclination}}.\end{aligned} \tag{17}$$

A generalized 3-D omnidirectional attenuation pattern model, which includes four attenuation factors, was first proposed as (17). In other words, the Maxwell formula was used to define attenuation function $F(R)_{\text{Lossy medium}}$ according to the lossy medium, while approximation model $F(R)_{\text{Radiation}}$ and bias factor $F(\phi)_{\text{Polarization}}$ were deduced according to the antenna effective area in the Friis formula. Finally, attenuation

Fig. 13. Experimental setup and equipment.

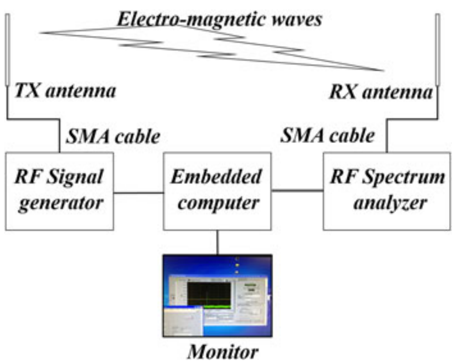

Fig. 14. Block diagram of transmitting and receiving node communication.

model $F(\Theta, \theta)_{\text{Elevation and Inclination}}$ according to the antenna position was combined to propose the generalized model for the 3-D omnidirectional antenna. In Section IV, an experiment conducted in an engineering basin environment to verify the proposed model is described.

IV. Experiment on Underwater Attenuation Pattern of Omnidirectional Antenna

A large anechoic room is required to determine a radiation pattern of antenna in air; however, an underwater experiment can be performed in a water bath of an appropriate size because electromagnetic waves are scarcely reflected on account of significant attenuation by the medium. In this study, the water bath and experimental equipment were arranged as shown in Figs. 13 and 14. A National Instruments 5660 vector spectrum analyzer and signal generator were employed. All experiments used the signal attenuation called received signal strength (RSS) unit of milliwatts, which appeared in the vector analyzer.

Characteristics of the experimental medium are shown in Table II. The performance of the omnidirectional antenna was measured in a nondirectional chamber of a professional institution, as shown in Fig. 15. The maximum directional gain of the antenna was determined to be 1.14 dBi.

A. Experiment on Position Loss Factor

Two attenuation factors based on the position and attitude between two nodes were mentioned in Section III-A for attenuation pattern analysis. Among them, $F(R)$ of the position loss factor was evaluated for attenuation characteristics in accordance with distance, as shown in Fig. 16. Antennas were fixed

TABLE II
Environmental Variables in Experiment Basin

	Property (symbol)	Characteristic value [unit]
Freshwater	Conductivity (σ)	0.075 [1/m]
	Permeability (μ)	1.2566×10^{-6} [Henry/m]
	Permittivity (ϵ)	7.2797×10^{-10} [F/m]
	Calibration factor (C_w)	-18.23 [dB]
Antenna	TX ant. gain in air G_T	0.14 [dBi]
	RX ant. gain in air G_R	0.14 [dBi]
	Transmission Power P_T	10 [mW]
	$D_{\max}$	1.3002
	HPBW	149.5272
	n	19.3709

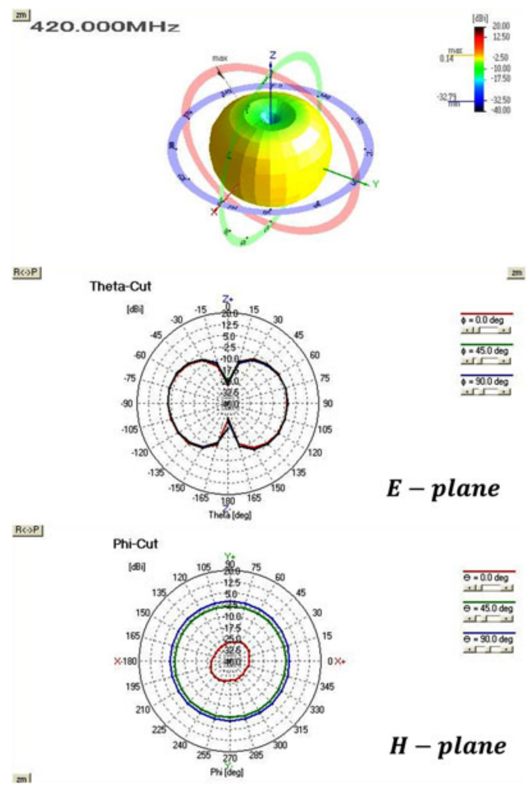

Fig. 15. Air experiment result of the dipole antenna by National Radio Research Agency.

Fig. 16. Experiment sets for $F(R)$: (a) experiment environment; (b) experiment diagram.

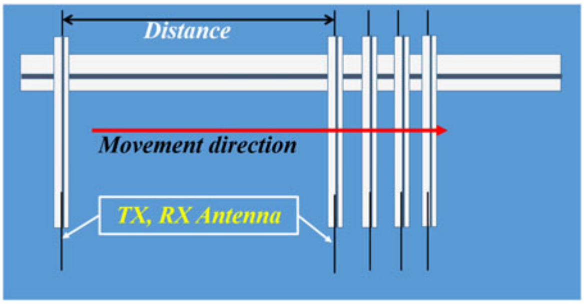

Fig. 17. Experiment result with calibration (dB scale) for $F(R)$.

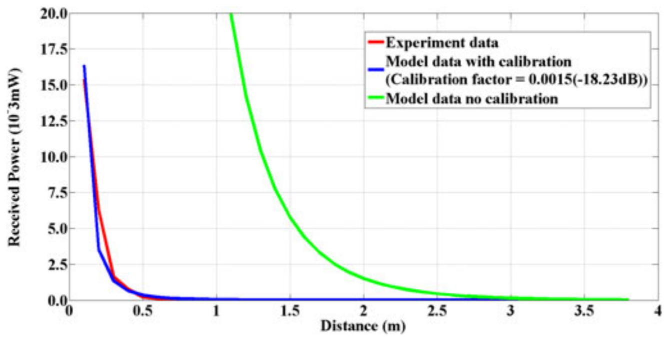

Fig. 18. Experiment sets for $F(\Theta)$: (a) experiment environment; (b) experiment diagram.

on a profile at a 1.5-m depth from the water surface; an antenna fixing frame was attached on top of the profile. Data of the reception signal intensity were obtained at a 10-cm interval. The results were obtained by averaging each set of 100 data items. They are shown in Fig. 16 as the reception signal intensity based on distance. Underwater distance calibration [14] was used to calibrate the variables for the medium.

From the experiment results, signal attenuation according to distance was verified to remain constant until the distance between the transmitting and receiving antennas exceeded 3 m. An existing calibration technique [14] was used to calibrate the difference from the theoretical model; the calibration result was indicated as blue line in Fig. 17. Because accurate values are unknown for the conductivity, permeability, and permittivity of the underwater medium, and for the reflection efficiency of the electromagnetic waves according to the medium, the calibration process was defined to combine them into a single variable and secure the result for distance estimation [14]. The underwater medium calibration variable (-18.23 dB $= 0.0015$) was confirmed; there was no environmental change according to the underwater medium variable compared to past studies. The attenuation model calibrated for the medium can be expressed as (18). After verifying the underwater medium variable, an experiment was conducted on elevation, inclination, and polarization of the antenna

$$\frac{P_R}{P_T} = 0.0015 \times e^{-\alpha R} \times \frac{\lambda^2}{(4\pi R)^2}. \tag{18}$$

The experimental sets shown in Fig. 18 were prepared to test the elevation loss factor based on the linear distance estimation model. HPBW and n of the omnidirectional antenna based on

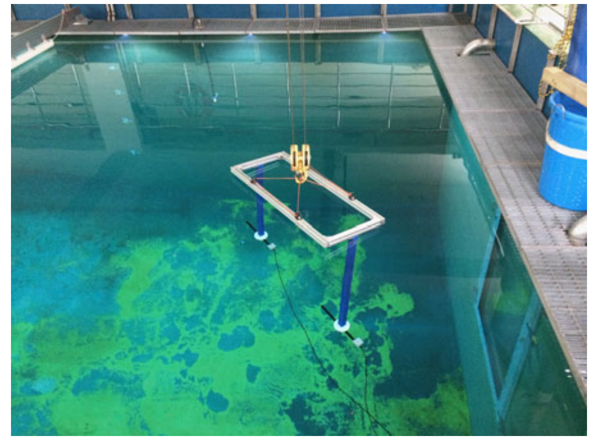

Fig. 19. Experiment results for $F(\Theta)$: (a) X, Y plot; (b) R, Θ polar expression.

the performance test result of Fig. 15 were found using the maximum directivity $D_{\max} = 1.3002$ which is given by the performance test. HPBW can be calculated by (7), and n is derived by (8) or (19) with HPBW. Then, HPBW $= 149.5272°$; $n = 19.3709$, respectively. Accordingly, the directivity model can be expressed as

$$0.5 = |\cos^n(\mathrm{HPBW}/2)| \tag{19}$$

$$D = 1.3002 \times \cos^{19.3709}(\Theta). \tag{20}$$

Fig. 19 shows how characteristics of the elevation loss factor appear with (11) and the gain of (20).

The experimental values according to rotation were obtained with an interval of 10° through the experimental sets shown in Fig. 18. Fig. 19 shows the experimental result and model estimation result in the form of a 2-D graph and polar coordinates. The result derived from the model shows clear intensity of the signal at 0° and 180°, which disappears at 90° and 270°. This attenuation pattern is similar to the generalized model like (17). In addition, there were some sections that showed irregular patterns in between them; nevertheless, the pattern of signal change was also similar to the theory. Irregular patterns were likely affected by the reflective, diffractive, and refractive characteristics of the antennas, as well as by interference waves generated by equipment near the experimental water bath.

B. Experiment of Attitude Loss Factor

The Friis formula defines attenuation according to the roll rotation between the antennas as the position loss factor [20]. The experimental sets were prepared as shown in Fig. 20 to experimentally test this in an underwater environment. The average reception signal intensity obtained from the rotation of the two antennas fixed to a frame, which could rotate 360° around the roll axis, is shown as a graph in Fig. 21.

Another factor relating to the antenna attitude is the inclination loss factor, which involves the rotation of the antenna around the pitch axis. The experiment for examining the effect of inclination loss factor $F(\theta)$ was performed as shown in Fig. 22. As verified in Fig. 23, the experimental result was also similar to the proposed model.

TABLE III
EXPERIMENTAL RESULTS IN 3-D POSITION

Node	Real Pos. (cm)	Model data (dBm) Ch. 0, 1 , 2 , 3	Exp. Data (dBm) Ch. 0, 1, 2, 3	Error (dB)	Distance error (cm)	STDEV. (dB)
YELLOW Node	(100, 100, 40)	−62.0558, −56.5059, −65.0335, −61.4826	−63.0089, −57.1476, −67.3657, −62.2256	−0.9530, −0.6687, −2.3321, −0.7430	1.1742	0.0339, 0.0167, 0.0551, 0.0304
PURPLE Node	(150, 50, 30)	−58.4685, −62.9924, −54.3400, −62.8136	−60,2957, −63.3337, −54.2055, −61.4354	−1.8272, −0.3413, −0.1345, 1.3783	0.7361	0.0246, 0.0343, 0.0127, 0.0262
RED Node	(150, 150, 20)	−64.3502, −72.1951, −58.9021, −69.4975	−63.3896, −74.4253, −58.1330, −71.5922	0.9606, −2.2302, 0.7691, −2.0947	2.9139	0.0370, 0.1307, 0.0195, 0.0861
GREEN Node	(150, 150, 50)	−72.1951, −64.3502, −69.4975, −58.9021	−74.8483, −62.9297, −71.5766, −59.5357	−2.6533, 1.4204, −2.0791, −0.6336	4.4301	0.1455, 0.0342, 0.0917, 0.0231
BLUE Node	(200, 150, 50)	−76.6124, −70.8262, −68.6429, −55.1643	−79.8487, −69.3012, −67.0314, −54.4534	−3.2363, 1.5251 1.6115, 0.7109	0.6863	0.2443, 0.0685, 0.0589, 0.0119

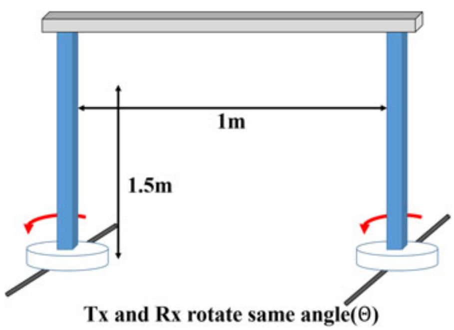

Fig. 20. Experiment sets for $F(\phi)$: (a) experiment environment; (b) experiment diagram.

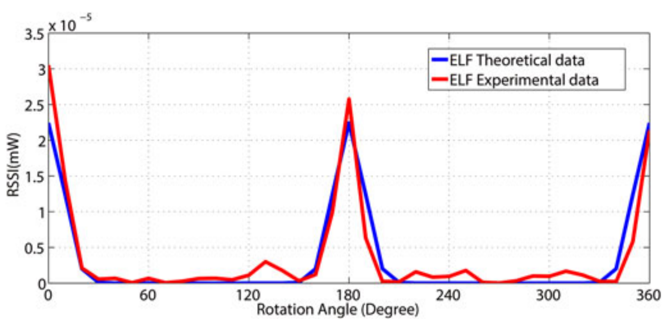

Fig. 21. Experimental result of PLF.

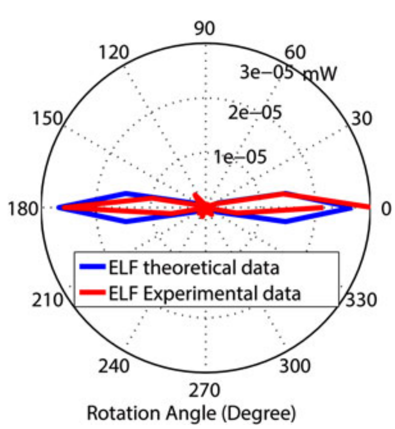

Fig. 22. Experiment sets for $F(\theta)$: (a) experiment environment; (b) experiment diagram.

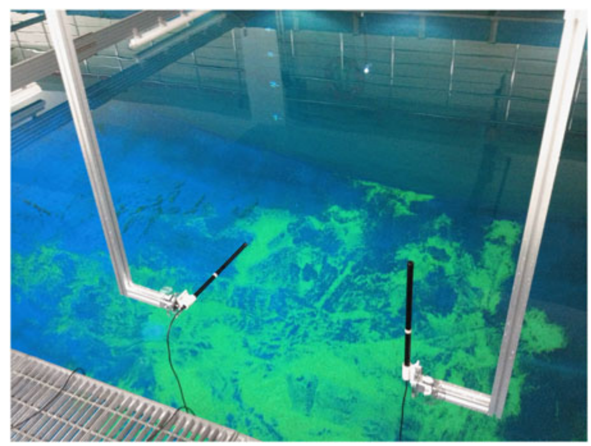

Fig. 23. Experiment results for $F(\theta)$: (a) X, Y plot; (b) R, θ polar expression.

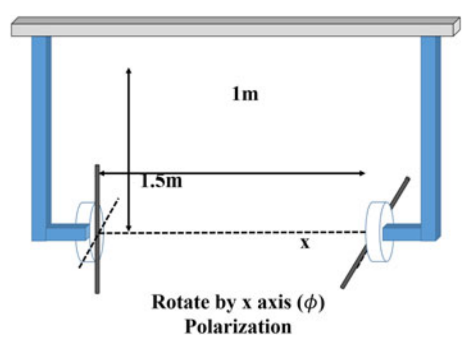

Fig. 24. Experimental set for static 3-D localization.

C. Experiment of Localization on Specific Points in Underwater 3-D Environment

As a result of antenna position experiment on Sections IV-A and IV-B, the position data from antenna position were verified. So this section shows that the feasibility of localization include 3-D static position using the theoretical model. For verifying generalized 3-D attenuation model, another experimental set was built as shown in Fig. 24. To verify the possibility of the proposed model as a 3-D localization system in underwater, we pick some test points for comparing the results by the proposed model with experimental results. We acquired the EM wave signals 160 times from four transmitting antennas to confirm the reliability for each point. Table III shows the experimental results. The standard deviation results show that the EM wave sensor is very reliable to use for distance measurement in 3-D environment, and the mean distance errors of each point show very small errors between calculated from the proposed model and measured by experiment. Finally, the proposed model could be used as a practical 3-D localization sensor.

V. Conclusion

In this paper, signal attenuation (received signal strength) of electromagnetic waves with an omnidirectional antenna in an underwater 3-D space was examined to establish an underwater 3-D localization system. The proposed method can be used to determine the distance between antennas defined as a fixed node and mobile node according to the degree of signal attenuation. An underwater position estimation system can be established based on the sensor network. In this paper, attenuation factors, which are based on the relative position and attitude between nodes, were defined as the position loss factor and attitude loss factor for the pattern modeling of an omnidirectional antenna in actual use. The position loss factor was defined as the distance, yaw angle, and elevation angle $(R, \varPhi, \varTheta)$ using the spherical coordinate. The attitude loss factor was defined as the roll, pitch, and yaw (ϕ, θ, ψ) using Euler angles. Among these factors, $\varPhi, \psi$ did not affect attenuation when omnidirectional antennas were used. Moreover, attenuation factors according to R and ϕ were systematically summarized using the plane wave equation and Friis formula. Because $\varTheta$, θ were affected by the pattern of the omnidirectional antenna on a vertical E-plane and showed a significant effect on attenuation, they were respectively redefined as the elevation loss factor and inclination loss factor. The E-plane characteristics of the omnidirectional antenna could be defined with McDonald approximation. This was used to apply the directivity of the individual antennas, for which detailed analysis was not provided by the Friis formula, and to derive the $F(R, \phi, \varTheta, \theta)$ model that affected the overall H- and E-plane domain. An attenuation model in 3-D space was proposed with consideration of all attenuation factors, and the validity of the model was demonstrated through experimentation. Especially, the feasibility of localization was verified by 3-D static position estimation using the theoretical model. We also plan to execute a real ROV maneuvering experiment using the proposed sensor system in near future.

Based on the theoretical model for an underwater 3-D omnidirectional antenna, an underwater 3-D position estimation system can be established using multiple fixed nodes and mobile nodes. In addition, the proposed attenuation model of electromagnetic waves is applicable to all antennas that allow for mathematical expression. It is additionally possible to expand this scope to all free and attenuation spaces.

References

[1] S.-C. Yu, J. Hyun, D.-Y. Kim, M.-K. Park, P. C. Cho, and C.-S. Hwang, "The development of multi-functional autonomous amphibious vehicle," in *Proc. IEEE Symp. Workshop Sci. Use Submarine Cables Related Technol. Underwater Technol.*, 2011, pp. 1–6.

[2] B.-H. Jun, J. Y. Park, P.-M. Lee, S.-J. Ma, Y. Kim, J.-H. Oh, and Y.-K. Lim, "Design, implementation and free running test of ISiMI; An AUV for cruising in ocean engineering basin environment," in *Proc. OCEANS Europe*, 2007, pp. 1–6.

[3] A. Palmeiro, M. Martín, I. Crowther, and M. Rhodes, "Underwater radio frequency communications," in *Proc. OCEANS, IEEE-Spain*, 2011, pp. 1–8.

[4] U. D. o. H. S. HOMEPORT. (2011, Mar.). Deepwater horizon the final report. [Online]. Available: https://homeport.uscg.mil/

[5] M. F. Fallon, J. Folkesson, H. McClelland, and J. J. Leonard, "Relocating underwater features autonomously using sonar-based SLAM," *IEEE J. Ocean. Eng.*, vol. 38, no. 3, pp. 500–513, Jul. 2013.

[6] L. Paull, S. Saeedi, M. Seto, and H. Li, "AUV navigation and localization: A review," *IEEE J. Ocean. Eng.*, vol. 39, no. 1, pp. 131–149, Jan. 2014.

[7] B. Zerr, G. Mailfert, A. Bertholom, and H. Ayreault, "Sidescan sonar image processing for AUV navigation," in *Proc. Oceans Europe*, 2005, vol. 1, pp. 124–130.

[8] S.-B. Han, J.-H. Kim, and H. Myung, "Landmark-based particle localization algorithm for mobile robots with a fish-eye vision system," *IEEE/ASME Trans. Mechatronics*, vol. 18, no. 6, pp. 1745–1756, Dec. 2013.

[9] D. Park, J. Kim, and W. K. Chung, "Simulated 3d underwater localization based on RF sensor model using EKF," in *Proc. 8th Int. Conf. Ubiquitous Robots Ambient Intell.*, 2011, pp. 832–833.

[10] X. Che, I. Wells, G. Dickers, P. Kear, and X. Gong, "Re-evaluation of RF electromagnetic communication in underwater sensor networks," *IEEE Commun. Mag.*, vol. 48, no. 12, pp. 143–151, Dec. 2010.

[11] A. I. Al-Shamma'a, A. Shaw, and S. Saman, "Propagation of electromagnetic waves at MHz frequencies through seawater," *IEEE Trans. Antennas Propag.*, vol. 52, no. 11, pp. 2843–2849, Nov. 2004.

[12] J. Lee and S. Nam, "Effective area of a receiving antenna in a lossy medium," *IEEE Trans. Antennas Propag.*, vol. 57, no. 6, pp. 1843–1845, Jun. 2009.

[13] S.-J. Lee, K. Kwak, and J. Kim, "Development of two dimensional underwater localization system using RF sensors," in *Proc. 7th Int. Conf. Ubiquitous Robots Ambient Intell.*, 2010, pp. 541–543.

[14] D. Park, K. Kwak, W. K. Chung, and J. Kim, "Development of underwater distance sensor using EM wave attenuation," in *Proc. IEEE Int. Conf. Robot. Autom.*, 2013, pp. 5125–5130.

[15] W. H. Hayt and J. A. Buck, *Engineering Electromagnetics*, vol. 7. New York, NY, USA: McGraw-Hill, 2001.

[16] A. Karlsson, "Physical limitations of antennas in a lossy medium," *IEEE Trans. Antennas Propag.*, vol. 52, no. 8, pp. 2027–2033, Aug. 2004.

[17] C. A. Balanis, *Antenna Theory: Analysis and Design*. Hoboken, NJ, USA: Wiley, 2012.

[18] L. J. Chu, "Physical limitations of omni-directional antennas," *J. Appl. Phys.*, vol. 19, no. 12, pp. 1163–1175, 1948.

[19] A. Boström, G. Kristensson, and S. Ström, "Transformation properties of plane, spherical and cylindrical scalar and vector wave functions," *Field Representations and Introduction to Scattering* (ser. Acoustic, Electromagnetic and Elastic Wave Scattering), vol. 1. Amsterdam, the Netherlands: North Holland, 1991, pp. 165–210.

[20] H. T. Friis, "Introduction to radio and radio antennas," *IEEE Spectrum*, vol. 8, no. 4, pp. 55–61, Apr. 1971.

Kyungmin Kwak (S'12) received the B.S. and M.S. degrees in mechanical engineering from the Seoul National University of Science and Technology, Seoul, Korea, in 2011 and 2013, respectively, where he is currently working toward the Ph.D. degree in mechanical and automotive engineering.

His current research interests include the areas of underwater localization, sensor network, and underwater robot design.

Daegil Park (S'12) received the B.S. degree in mechanical engineering from the Seoul National University of Science and Technology, Seoul, Korea, in 2011. He is currently working toward the M.S. and Ph.D. degrees in mechanical engineering at the Pohang University of Science and Technology, Pohang, Korea.

His current research interests include the areas of marine robots, underwater sensor networks, distributed robots, and localization.

Wan Kyun Chung (S'84–M'86–F'16) received the B.S. degree in mechanical design from Seoul National University, Seoul, Korea, in 1981, and the M.S. degree in mechanical engineering and the Ph.D. degree in production engineering from the Korea Advanced Institute of Science and Technology, Daejeon, Korea, in 1983 and 1987, respectively.

He is currently a Professor at the School of Mechanical Engineering, Pohang University of Science and Technology, Pohang, Korea (he joined the faculty in 1987). In 1988, he was a Visiting Professor with the Robotics Institute, Carnegie Mellon University, Pittsburgh, PA, USA. In 1995, he was a Visiting Scholar with the University of California Berkeley, Berkeley, CA, USA. His research interests include development of robust controllers for precision motion control, biomedical robotics, and underwater robots.

Prof. Chung served as a Senior Editor for the IEEE TRANSACTIONS ON ROBOTICS and he is serving as a Senior Editor for the IEEE ROBOTICS AND AUTOMATION LETTERS, and a Regional Editor for the *Journal of Intelligent Service Robotics.*

Jinhyun Kim (S'03–M'05) received the B.S., M.S., and Ph.D. degrees in mechanical engineering from the Pohang University of Science and Technology, Pohang, Korea, in 1998, 2000, and 2005, respectively.

He was a Senior Engineer with the Korea Institute of Industrial Technology, Ansan, Korea, during 2005–2007. In 2007, he joined the Seoul National University of Science and Technology, Seoul, Korea, where he is currently a Professor at the Department of Mechanical Engineering. In 2013, he was a Visiting Professor with the Department of Mechanical Engineering, University of Washington, Seattle, WA, USA. His current research interests include the areas of redundant manipulators, marine robots, hovering robots, and neurorobotics.

Prof. Kim is an Associate Editor of the *Journal of Intelligent Service Robotics*.